Ultra-low-dose chest computed tomography for interstitial lung disease using model-based iterative reconstruction with or without the lung setting

Akinori Hata, MD, PhD*, Masahiro Yanagawa, MD, PhD, Osamu Honda, MD, PhD, Tomo Miyata, MD, Noriyuki Tomiyama, MD, PhD

Abstract

Objectives: The aim of this study was to assess the effects of reconstruction on the image quality and quantitative analysis for interstitial lung disease (ILD) using filtered back projection (FBP) and model-based iterative reconstruction (MBIR) with the lung setting and the conventional setting on ultra-low-dose computed tomography (CT).

Methods: Fifty-two patients with known ILD were prospectively enrolled and underwent CT at an ultra-low dose (0.18 ± 0.02 mSv) and a standard dose (7.01 ± 2.66 mSv). Ultra-low-dose CT was reconstructed using FBP (uFBP) and MBIR with the lung setting (uMBIR-Lung) and the conventional setting (uMBIR-Stnd). Standard-dose CT was reconstructed using FBP (sFBP). Three radiologists subjectively evaluated the images on a 3-point scale (1 = worst, 3 = best). For objective image quality analysis, regions of interest were placed in the lung parenchyma and the axillary fat, and standard deviation (SD), signal-to-noise ratio (SNR), and contrast-to-noise ratio (CNR) were evaluated. For 32 patients with clinically diagnosed idiopathic interstitial pneumonia, quantitative measurements including total lung volume (TLV) and the percentage of ILD volume (%ILDV) were obtained. The medians of 3 radiologists' scores were analyzed using the Wilcoxon signed-rank test and the objective noise was analyzed using the paired t test. The Bonferroni correction was used for multiple comparisons. The quantitative measurements were analyzed using the Bland-Altman method.

Results: uMBIR-Lung scored better than uMBIR-Stnd and worse than sFBP ($P < .001$), except for noise and streak artifact in subjective analysis. The SD decreased significantly in the order of uMBIR-Stnd, uMBIR-Lung, sFBP, and uFBP ($P < .001$). The SNR and CNR increased significantly in the order of uMBIR-Stnd, uMBIR-Lung, sFBP, and uFBP ($P < .001$). For TLV, there was no significant bias between ultra-low-dose MBIRs and sFBP ($P > .3$). For %ILDV, there was no significant bias between uMBIR-Lung and sFBP (p = 0.8), but uMBIR-Stnd showed significantly lower %ILDV than sFBP ($P = .013$).

Conclusions: uMBIR-Lung provided more appropriate image quality than uMBIR-Stnd. Although inferior to standard-dose CT for image quality, uMBIR-Lung showed equivalent CT quantitative measurements to standard-dose CT.

Abbreviations: %ILDV = percentage of interstitial lung disease volume, BMI = body mass index, CT = computed tomography, DLP = dose-length product, ED = effective dose, FBP = filtered back projection, HU = hounsfield units, ILD = interstitial lung disease, IPF = idiopathic pulmonary fibrosis, IR = iterative reconstruction, MBIR = model-based iterative reconstruction, ROI = region of interest, SD = standard deviation, sFBP = FBP on standard-dose CT, TLV = total lung volume, uFBP = FBP on ultra-low-dose CT, uMBIR-Lung = MBIR with the lung setting on ultra-low-dose CT, uMBIR-Stnd = MBIR with the conventional setting on ultra-low-dose CT.

Keywords: computer-assisted, image processing, image reconstruction, interstitial lung diseases, multidetector computed tomography, radiation dosage

1. Introduction

As the use of computed tomography (CT) grows, medical radiation exposure has increased worldwide. Consequently, concerns about the risk of cancer induced by radiation have also increased. Recently, iterative reconstruction (IR) algorithms have been available in the clinical setting and contribute to dose reduction without degradation of image quality.

Model-based iterative reconstruction (MBIR) is a recent pure IR technique, and it considers system statistics and system optics. MBIR is mathematically complex and time-consuming, but many studies have reported its usefulness in various body regions.[1–11] It has been generally reported that compared with traditional FBP, MBIR achieves CT images with less noise, improved spatial resolution, and increased contrast resolution.[12] Although the previous generation of MBIR had no option for specific body regions, the latest generation of MBIR has some clinical settings for the head, lung, and abdomen.[13,14] Several studies reported that the latest-generation MBIR with the lung setting could provide higher resolution images and more appropriate image quality for lung assessment than the conventional setting that has the same physical characteristics as previous generation of MBIR.[13,14]

Recent advances in IR technique have enabled ultra-low-dose CT, whose radiation dose is equivalent to chest x-ray.[15–18] Wang et al[15] reported that ultra-low-dose chest CT with an effective dose of 0.13 mSv could be used for quantification of lung density and for detecting emphysema. Messerli et al[16] also reported that ultra-low-dose CT was useful for pulmonary nodule detection. IR technique contributed to the results in these studies. However, few studies have investigated the effect of the latest generation of MBIR with the lung setting on ultra-low-dose CT of patients with interstitial lung disease (ILD).

For the assessment of ILD, visual evaluation of CT scans is used clinically to evaluate the pattern and extent of lung changes. In addition, quantitative CT evaluation has been proposed as a method for the evaluation of ILD.[19–23] Density mask technique using CT attenuation thresholds has been reported to demonstrate good correlation with pulmonary function test or CT visual scores in patients with idiopathic interstitial pneumonia.[20] This quantitative measurement enables us to evaluate ILD without intra- and interobserver variabilities, as found with visual assessment.

The purpose of this study was to assess the effects of reconstruction on the image quality and the CT quantitative measurements of ultra-low-dose chest CT for patients with ILD using filtered back projection (FBP) and the latest generation of MBIR.

2. Materials and methods

2.1. Patients

Our institutional review board approved this prospective, observational, and single-center study, and 52 patients were recruited. Patients were identified from referral to the department for a non-contrast chest CT specifically for follow-up of previously detected ILD findings from January 2016 to February 2017. The inclusion criteria were age ≥40 years at the time of the scan and able to provide written, informed consent. Exclusion criteria were unable to give inform consent and pregnancy. All patients provided written, informed consent and underwent ultra-low-dose CT in addition to standard-dose CT for clinical purposes. Age, body mass index (BMI), and clinical diagnosis of ILD were recorded.

2.2. CT acquisition and image reconstruction

A multidetector row CT scanner (Discovery CT750HD; GE Healthcare Technologies, Milwaukee, WI) was used in this study. The patients underwent 2 of repeated scans without contrast enhancement. A standard-dose CT was performed, and then ultra-low-dose CT was performed immediately after standard-dose CT, but with a separate breath-hold. The standard-dose CT was performed using routine clinical protocol with tube current modulation based on a fixed noise index (11.50). The ultra-low-dose CT was performed with 10 mA for tube current. The other CT parameters for both standard-dose and ultra-low-dose CT were as follows: detector collimation, 0.625 mm; detector pitch, 0.984; gantry rotation period, 0.4 seconds; x-ray voltage, 120 kVp; non-high resolution mode with 984 views per rotation. All scans were performed with the patient in a supine position at end-inspiration. CT dose index volume (CTDIvol) and dose-length product (DLP) were recorded for all scans. Effective dose (ED) was calculated as the product of DLP and the "k" conversion coefficient (0.014 mSv/mGy cm) for chest CT.[24]

Axial thin-section images with thickness of 0.625 mm, matrix size of 512×512, and field of view of 34.5 cm were reconstructed on ultra-low-dose CT. Veo 3.0 (GE Healthcare Technologies), which was one of the latest-generation MBIRs, was used. Veo 3.0 had some setting options for reconstruction: Stnd setting was a conventional setting that had the same physical characteristics as Veo 2.0 (previous generation of MBIR and previous version of Veo 3.0); and RP20 setting was one of the lung settings prepared to provide high-resolution images.[14] Ultra-low-dose CT was reconstructed using FBP with sharp kernel (uFBP), MBIR with the RP20 setting (uMBIR-Lung), and MBIR with the Stnd setting (uMBIR-Stnd). Standard-dose CT was reconstructed using FBP with sharp kernel (sFBP) at the same section thickness, matrix size, and field of view. In total, 4 data sets of CT images (sFBP, uFBP, uMBIR-Lung, and uMBIR-Stnd) were obtained for each patient.

The principal investigator (A.H., with 8 years of experience) chose the images for evaluation at the carina level and lung base level. In addition, images in which the most conspicuous CT findings were found were also chosen for evaluation from each CT data set. The CT findings were bronchiectasis, reticulation, ground-glass opacity (GGO), and honeycombing. Totally, 6 image sets for evaluation (carina-level images, lung-base-level images, bronchiectasis images, reticulation images, GGO images, and honeycombing images) for each reconstruction (sFBP, uFBP, uMBIR-Lung, and uMBIR-Stnd) were obtained. As reference standards, a carina-level image, a lung base-level image, and an image for each CT finding were chosen from uMBIR-Lung cases. The reference standard images were selected at different levels from the evaluation images.

2.3. Subjective image analysis

Three chest radiologists (O.H., M.Y., and T.M., with 26, 17, and 6 years of experience, respectively) independently analyzed the evaluation images on a 3-megapixel 21-inch monochrome liquid crystal display monitor. All images were displayed at a window level of -700 HU and a window width of 1200 HU. The observers

were blinded to the CT protocol and image reconstruction of each image. The observers compared each evaluation image with reference standard images. Noise, streak artifact, blurring of the border between the lung and chest wall, clarity of small vessels, and overall image quality of the carina-level and lung base-level images were graded using a 3-point scale: 3 = superior to the reference standard image; 2 = almost equal to the reference standard image; and 1 = inferior to the reference standard image. The CT findings were also graded based on the above-mentioned 3-point scale.

2.4. Objective image quality

The signal (mean CT value, HU) and noise (standard deviation, SD) were evaluated quantitatively within a region of interest (ROI), which was defined by a cursor using image-processing software (ImageJ version 1.49 v; NIH, Bethesda, MD).[25] In the images at the carina level, ROIs, 10 mm in diameter, were placed in the uniform region in the lung parenchyma and axillary fat. The ROIs were placed at exactly the same location among the 4 reconstructions (sFBP, uFBP, uMBIR-Lung, and uMBIR-Stnd). The signal-to-noise ratio (SNR) was defined as mean CT value divided by SD in the ROI of the lung parenchyma. The contrast-to-noise ratio (CNR) was calculated by dividing the absolute difference of the attenuations between lung parenchyma and axillary fat by the image noise of axillary fat.

2.5. CT quantitative analysis

CT quantitative analysis was applied to the patients with idiopathic interstitial pneumonia. The patients with the other ILDs were excluded from this analysis, because it was controversial to apply this analysis to non-idiopathic interstitial pneumonia. A commercial workstation (ZIOSTATION; Ziosoft, Osaka, Japan) was used for analysis and a semiautomatic procedure was performed to segment the lung parenchyma from the surrounding tissue using the whole lung image. First, the principal investigator pointed the lung area, and then lung region with airway was segmented. Second, the airway (trachea and major bronchi) was segmented automatically. Finally, airway segmentation was excluded from the lung with airway segmentation, and lung parenchyma segmentation was obtained. This semiautomatic segmentation was performed using image sets of sFBP, uFBP, uMBIR-Lung, and uMBIR-Stnd. No manual segmentation and no correction of segmentation were performed. From the successful segmented lung parenchyma, total lung volume (TLV) was obtained. In reference to previous study,[20] the volume with attenuations between −500 and −700 Hounsfield Unit (HU) was defined as ILD volume (ILDV) and the ratios of ILDV to TLV was designated as %ILDV.

2.6. Statistical analysis

All statistical analyses were performed using SPSS for Windows Version 23 (IBM Corp., Armonk, NY). For the subjective analysis, the median values of the scores of the 3 observers were analyzed statistically. Differences in the median scores among the 4 reconstructions were assessed with the Wilcoxon signed rank test, which was conducted with Bonferroni correction for multiple comparisons. For objective image quality analysis, the differences of average SD values, SNR, and CNR were assessed with the paired t test with Bonferroni correction. A Bonferroni-corrected P value of

<0.0083 (0.05/6) was considered significant. The Bland-Altman analyses were performed to evaluate the differences in TLV and % ILDV between standard-dose CT (sFBP) and ultra-low-dose MBIRs (uMBIR-Lung and uMBIR-Stnd). The measurements for uFBP were excluded from this analysis because the segmentation for uFBP was successful in only 10 cases. The limit of agreement was calculated by multiplying the SD of the difference of each measurement by 1.96. The bias was assessed with t test, and the P value of <.05 was considered significant.

3. Results

3.1. Patients' demographics and radiation dose

The patients' demographics were as follows: 29 men and 23 women; mean age, 71.4 years (range, 48–89 years); and mean BMI 22.8 kg/m^2 (range, 16.2–32.5 kg/m^2). A total of 15 patients had collagen-vascular disease-associated ILD, 3 patients had anti-neutrophil cytoplasmic antibody (ANCA)-associated vasculitis-associated ILD, 2 patients had chronic hypersensitivity pneumonitis, and 32 patients were clinically diagnosed as having idiopathic interstitial pneumonia. Among the patients with collagen-vascular diseases, 8 patients had rheumatoid arthritis, 2 patients had Sjögren syndrome, and 2 patients had systemic sclerosis. Three patients had multiple collagen-vascular diseases including rheumatoid arthritis, Sjögren syndrome, systemic sclerosis, polymyositis, and ankylosing spondylitis. Among the patients with idiopathic interstitial pneumonia, 1 patient had idiopathic pulmonary fibrosis (IPF) that was proven pathologically. Sixteen patients were diagnosed as idiopathic nonspecific interstitial pneumonia, and 15 patients were diagnosed as IPF from clinical information and radiologic features. The flowchart of enrolled patients and our procedures is shown in Figure 1.

The CTDIvol, DLP, and ED were 12.79 ± 4.44 mGy, 500.75 ± 190.11 mGy-cm, and 7.01 ± 2.66 mSv, respectively, for standard-dose CT and 0.33 ± 0.03 mGy, 12.82 ± 1.62 mGy-cm, and 0.18 ± 0.02 mSv, respectively, for ultra-low-dose CT.

3.2. Subjective image analysis

The scores for the subjective analysis are summarized in Table 1. The scores of uMBIR-Lung were significantly better than those of uMBIR-Stnd in terms of blurring of the border between the lung and chest wall, clarity of small vessels, and overall image quality (all P values < .001) at both the carina and lung base levels (Fig. 2). In terms of noise ($P < .001$) and streak artifact ($P < .01$), the score of uMBIR-Stnd was significantly better than that of uMBIR-Lung at both levels. uMBIR-Lung performed better than uFBP for all items (all P values < .001), and uMBIR-Stnd performed better than uFBP, except for blurring of the border between the lung and chest wall and overall image quality. Both uMBIR-Lung and uMBIR-Stnd performed worse than sFBP in terms of blurring of the border between the lung and chest wall, clarity of small vessels, and overall image quality (all P values < .001), and they performed better than sFBP in terms of noise and streak artifact at both levels (all P values < .001).

As for CT findings, the scores of uMBIR-Lung were significantly better than of uMBIR-Stnd and uFBP for all items (all P values < .001; Fig. 3). uMBIR-Stnd performed better than uFBP only in terms of ground-glass opacity. Both uMBIR-Stnd and uMBIR-Lung performed worse than sFBP for all CT findings ($P < .001$; Fig. 4).
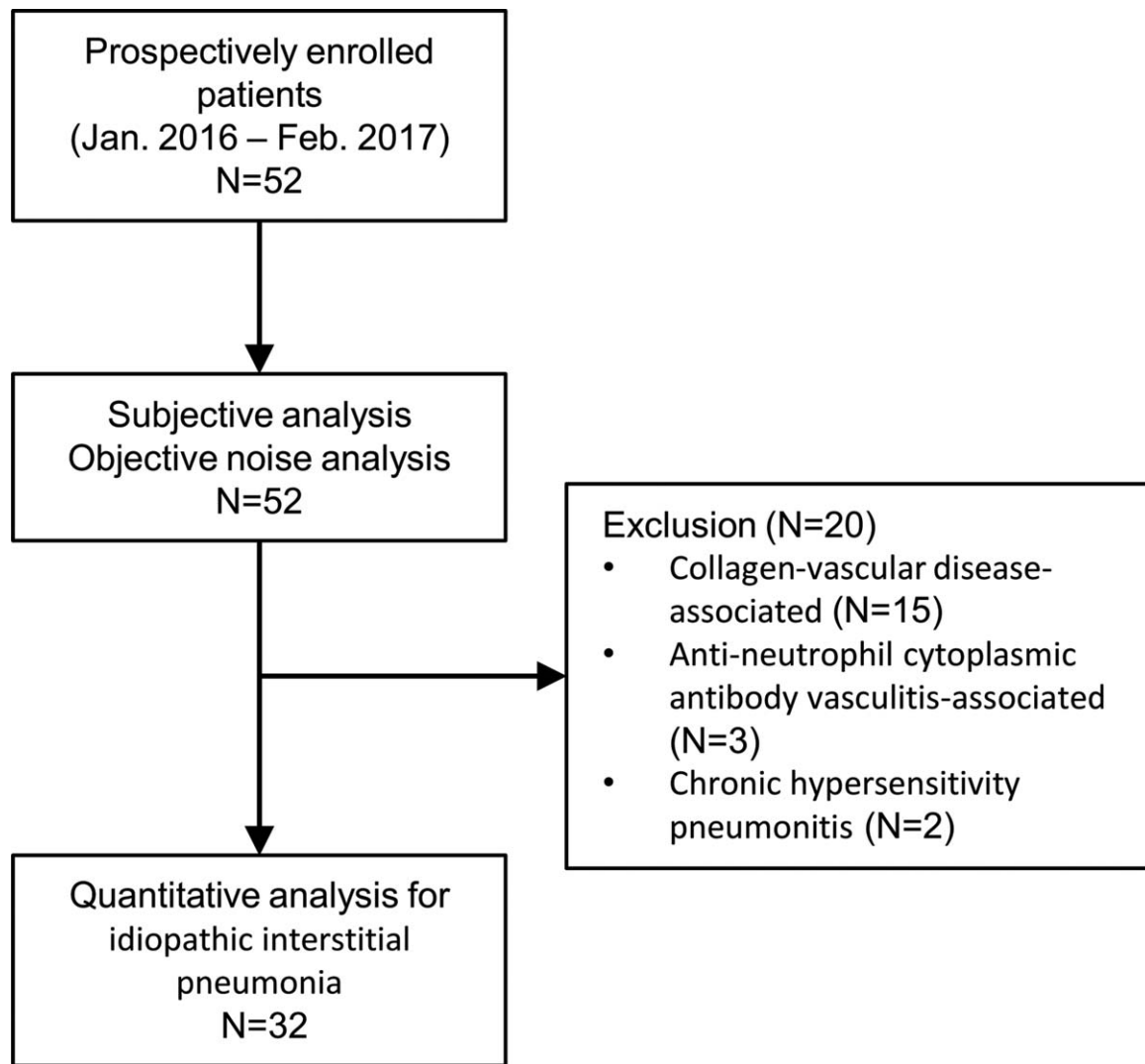
Figure 1. Flowchart of enrolled patients and our procedure.

3.3. Objective image quality

The objective image measurements are summarized in Table 2. The SD decreased significantly in the order of uMBIR-Stnd, uMBIR-Lung, sFBP, and uFBP ($P < .001$). The SNR and CNR increased significantly in the order of uMBIR-Stnd, uMBIR-Lung, sFBP, and uFBP ($P < .001$).

3.4. CT quantitative analysis

CT quantitative analyses were performed in 32 cases with idiopathic interstitial pneumonia. Among the 32 cases, the segmentation was successful in 10 patients using uFBP. Almost no lung area was segmented in 22 cases using uFBP. The lung segmentation was successful in all 32 cases using sFBP, uMBIR-Lung, and uMBIR-Stnd. The results of quantifications and Bland-Altman analysis are summarized in Table 3 and Figure 5. uMBIR-Lung showed no significant bias in both TLV ($P = .31$) and % ILDV ($P = .80$) compared with sFBP. uMBIR-Stnd showed no significant bias in TLV (p = .59), but for %ILDV, there was significant bias between uMBIR-Stnd and sFBP (p = .013). The

bias and limits of agreement of uMBIR-Lung tended to be smaller than those of uMBIR-Stnd (Fig. 5).

4. Discussion

The present results showed that the image quality of MBIR with the lung setting was better than that of MBIR with the conventional setting on ultra-low-dose CT, except for noise and streak artifact. The noise of MBIR with the conventional setting was significantly less than that of MBIR with the lung setting. In traditional FBP, the high-resolution algorithm is accompanied by an increase in noise, but it has been reported to be useful for lung assessment.[26,27] The present results suggest that the lung setting of MBIR may provide more appropriate images for lung assessment than the conventional setting on ultra-low-dose CT. MBIRs on ultra-low-dose CT performed worse than FBP on standard-dose CT, except for noise and streak artifact, but MBIR with the lung setting showed smaller biases and limit of agreement than MBIR with the conventional setting and equivalent %ILDV to standard-dose CT.

Table 1

Comparisons of subjective scores among standard-dose FBP, ultra-low-dose FBP, ultra-low dose MBIR-Lung, and ultra-low-dose MBIR-Stnd.

|	Carina level					Lung base level					CT findings			
	Noise	Streak artifact	Blurring	Small vessel clarity	Overall image quality	Noise	Streak artifact	Blurring	Small vessel clarity	Overall image quality	Bronchi-ectasis	Reticu-lation	Ground-glass opacity	Honey-combing
Subjective score														
sFBP	1.1±0.3	1.1±0.3	3.0±0.2	2.9±0.4	3.0±0.0	1.0±0.0	1.0±0.1	3.0±0.0	2.9±0.3	3.0±0.0	2.5±0.5	2.7±0.5	2.8±0.4	3.0±0.0
uFBP	1.0±0.0	1.0±0.0	1.3±0.5	1.0±0.1	1.0±0.0	1.0±0.0	1.0±0.0	1.4±0.6	1.1±0.2	1.0±0.0	1.0±0.0	1.1±0.2	1.0±0.0	1.1±0.3
uMBIR-Lung	2.0±0.0	2.0±0.0	1.7±0.5	1.5±0.5	1.4±0.5	2.0±0.2	2.0±0.0	2.3±0.5	1.7±0.6	2.1±0.5	1.4±0.5	1.8±0.6	2.0±0.2	2.0±0.6
uMBI-Stnd	2.4±0.5	2.1±0.3	1.2±0.4	1.3±0.5	1.1±0.3	2.9±0.3	2.9±0.3	1.9±0.6	1.3±0.5	1.5±0.7	1.1±0.3	1.2±0.4	1.4±0.5	1.2±0.5
Statistical analysis														
sFBP vs uFBP	0.008*	0.025	<.001*	<.001*	<.001*	1.000	0.317	<.001*	<.001*	<.001*	<.001*	<.001*	<.001*	<.001*
sFBP vs uMBIR-Lung	<.001*	<.001*	<.001*	<.001*	<.001*	<.001*	<.001*	<.001*	<.001*	<.001*	<.001*	<.001*	<.001*	<.001*
sFBP vs uMBIR-Stnd	<.001*	<.001*	<.001*	<.001*	<.001*	<.001*	<.001*	<.001*	<.001*	<.001*	<.001*	<.001*	<.001*	<.001*
uFBP vs uMBIR-Lung	<.001*	<.001*	<.001*	<.001*	<.001*	<.001*	<.001*	<.001*	<.001*	<.001*	<.001*	<.001*	<.001*	<.001*
uFBP vs uMBIR-Stnd	<.001*	<.001*	0.035	<.001*	0.025	<.001*	<.001*	<.001*	0.004*	<.001*	0.025	0.058	<.001*	0.564
uMBIR-Lung vs uMBIR-Stnd	<.001*	0.008*	<.001*	<.001*	<.001*	<.001*	<.001*	<.001*	<.001*	<.001*	<.001*	<.001*	<.001*	<.001*

FBP = filtered back projection, MBIR = model-based iterative reconstruction, sFBP = FBP on standard dose CT, uFBP = FBP on ultra-low dose CT, uMBIR-Lung = MBIR with lung setting on ultra-low dose CT, uMBIR-Stnd = MBIR with conventional setting on ultra-low dose CT.

Subjective analysis scores are expressed as mean ± standard deviation.

* A Bonferroni-corrected P value <.0083 was considered significant in statistical analysis.
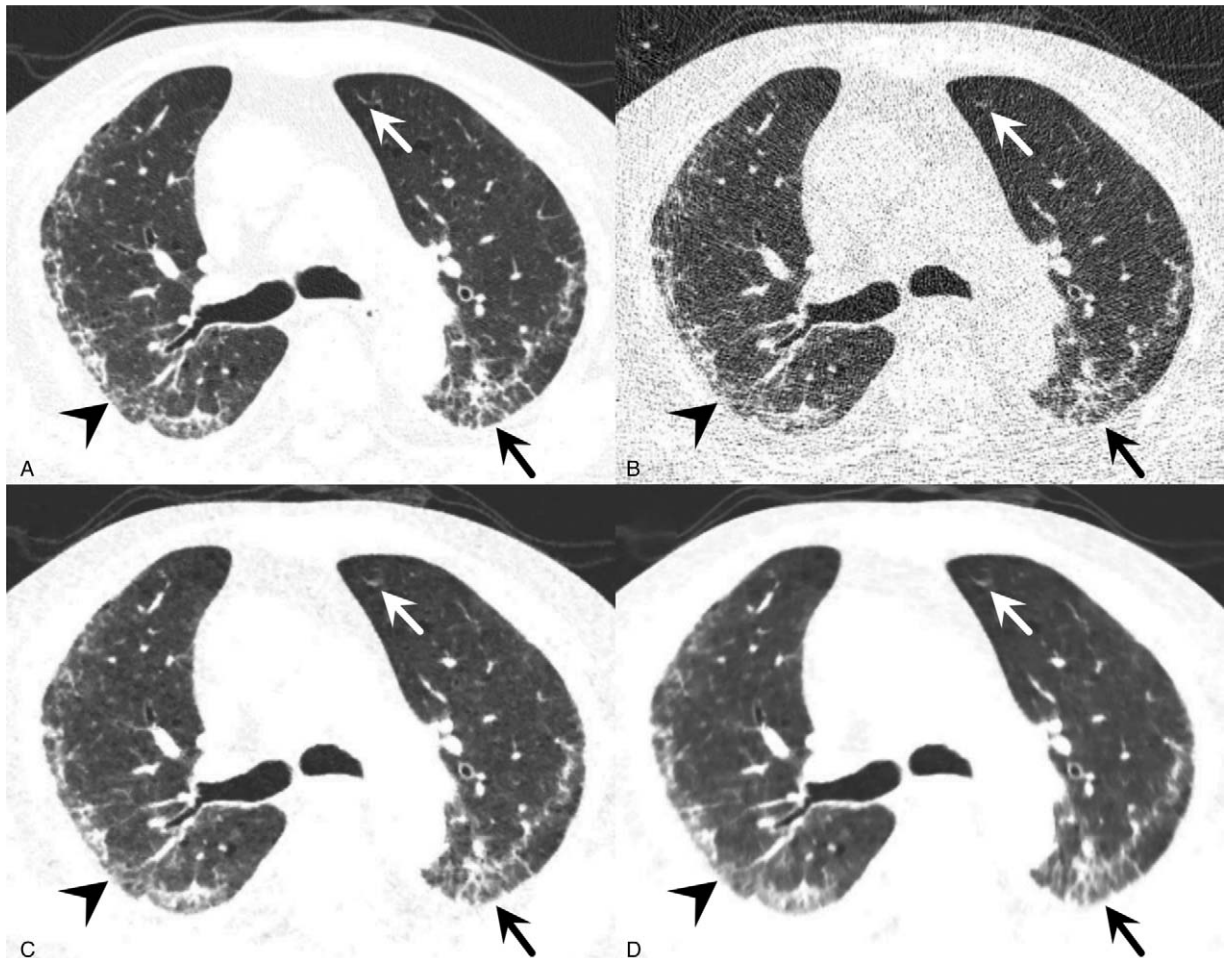
Figure 2. A 72-year-old woman with collagen vascular diseases (systemic sclerosis and polymyositis). Body mass index was 19.2 kg/m². Axial images at the carina level reconstructed using FBP on standard-dose CT (A), FBP on ultra-low-dose CT (B), MBIR with the lung setting (C), and MBIR with the conventional setting (D). Ground-glass opacity (arrowheads) is depicted more clearly on MBIR with the lung setting compared with the conventional setting, but they are slightly blurred compared with FBP on standard-dose CT. The border between the lung and chest wall (black arrows) is blurred on MBIR with the conventional setting. The noise of MBIR with the conventional setting is less than that with the lung setting. FBP on ultra-low-dose CT shows poor image quality with much noise and streak artifact. CT = computed tomography, FBP = filtered back projection, MBIR = model-based iterative reconstruction.
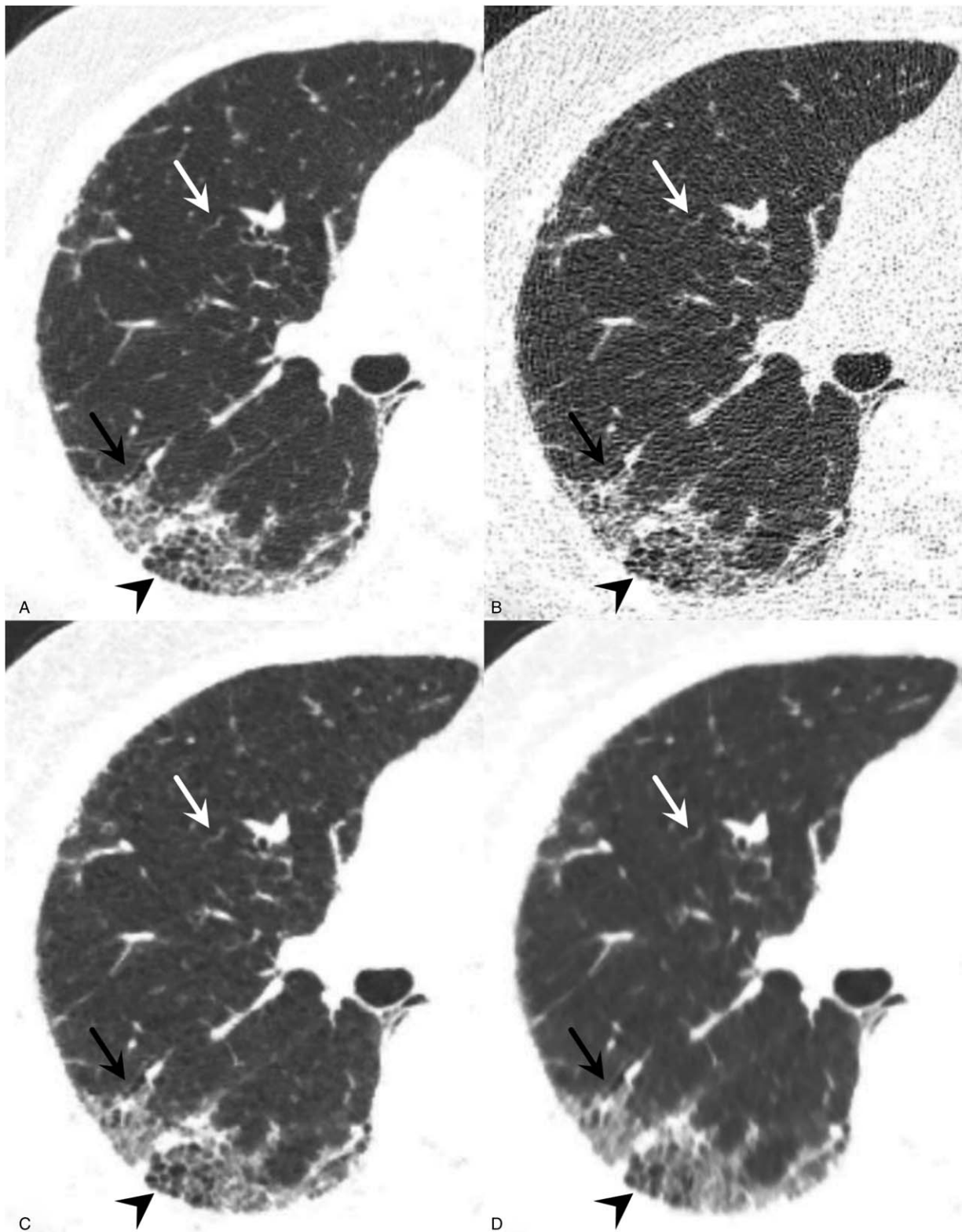
Figure 3. A 66-year-old man with idiopathic interstitial pneumonia (usual interstitial pneumonia pattern). Body mass index was 22.2 kg/m^2. Axial images using FBP on standard-dose CT (A), FBP on ultra-low-dose CT (B), MBIR with the lung setting (C), and MBIR with the conventional setting (D). Bronchiectasis (black arrows), reticulation (arrowheads), and small vessels (white arrows) are depicted more clearly on MBIR with the lung setting than with the conventional setting. They are depicted similarly using FBP on standard-dose CT and MBIR with the lung setting. CT = computed tomography, FBP = filtered back projection, MBIR = model-based iterative reconstruction.
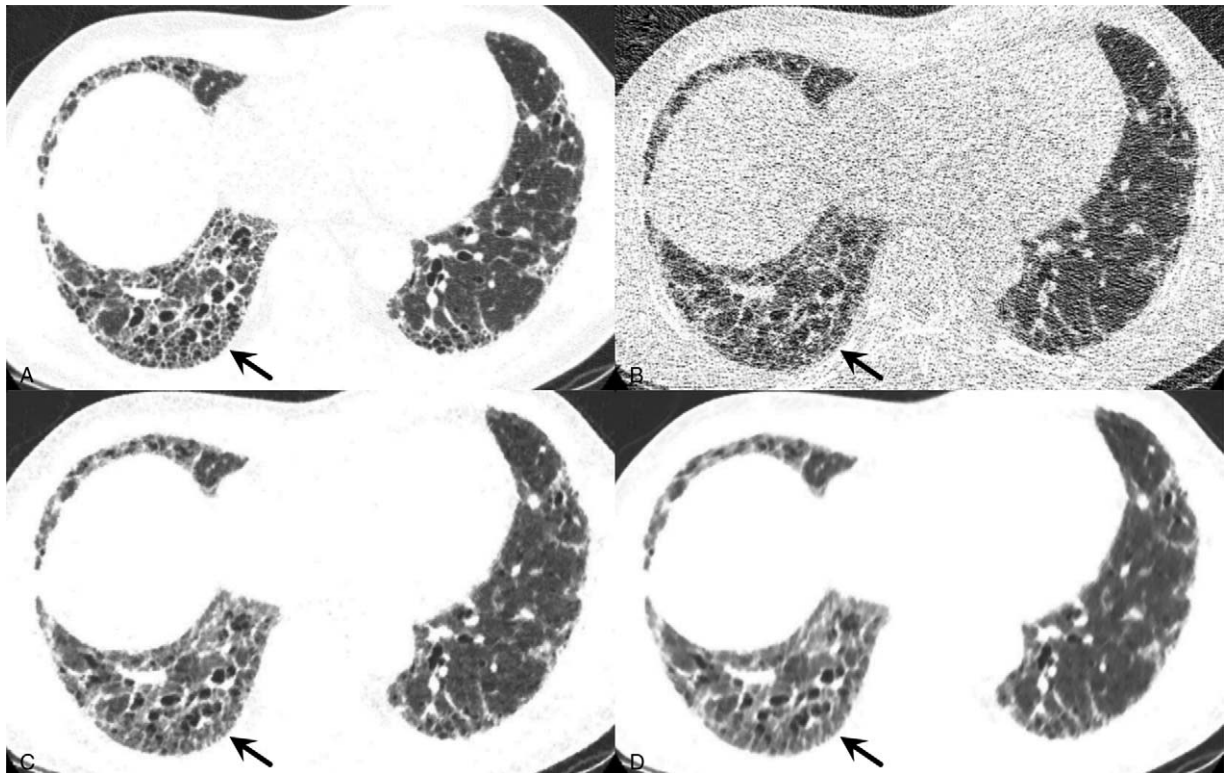
Figure 4. A 73-year-old woman with idiopathic interstitial pneumonia (usual interstitial pneumonia pattern). Body mass index was 19.7 kg/m². Axial images using FBP on standard-dose CT (A), FBP on ultra-low-dose CT (B), MBIR with the lung setting (C), and MBIR with the conventional setting (D). Small honeycombing is detectable on the FBP image on standard-dose CT, but it is difficult to see on ultra-low-dose CT images (arrows). CT = computed tomography, FBP = filtered back projection, MBIR = model-based iterative reconstruction.

The previous generation of MBIR was reported to have a unique feature called pixelated blotchy appearance.[1,2] This feature resulted in a step-like appearance at the interface of tissues or blurring of subtle structures. Padole et al[28] reported that MBIR images on sub-mSv CT were suboptimal for evaluation of

visibility of normal structures of the lung. Yanagawa et al[3] also reported that MBIR images on ultra-low-dose CT may decrease the visibility of fine and low-contrast abnormalities such as intralobular reticular opacities. The present study showed that the lung setting of the latest generation MBIR improved small vessel clarity, blurring of the border of lung and chest wall, and CT findings of ILD, even on ultra-low-dose

Table 2

Comparison of objective values among standard dose FBP, ultra-low dose FBP, ultra-low dose MBIR-Stnd, and ultra-low dose MBIR-Lung.

	SD (HU)	SNR	CNR
Objective value			
sFBP	48.0 ± 9.8	19.3 ± 4.6	17.7 ± 2.2
uFBP	202.6 ± 62.8	4.7 ± 1.2	3.3 ± 0.9
uMBIR-Stnd	23.1 ± 4.9	39.4 ± 6.2	49.6 ± 9.1
uMBIR-Lung	39.9 ± 6.6	22.8 ± 4.0	20.4 ± 3.5
Statiscal analysis			
sFBP vs uFBP	<.001*	<.001*	<.001*
sFBP vs uMBIR-Stnd	<.001*	<.001*	<.001*
sFBP vs uMBIR-Lung	<.001*	<.001*	<.001*
uFBP vs uMBIR-Stnd	<.001*	<.001*	<.001*
uFBP vs uMBIR-Lung	<.001*	<.001*	<.001*
uMBIR-Stnd vs uMBIR-lung	<.001*	<.001*	<.001*

CNR = contrast-to-noise ratio, FBP = filtered back projection, MBIR = model-based iterative reconstruction, SD = standard deviation, sFBP = FBP on standard dose CT, SNR = signal-to-noise ratio, uFBP = FBP on ultra low dose CT, uMBIR-Lung = MBIR with lung setting on ultra low dose CT, uMBIR-Stnd = MBIR with conventional setting on ultra-low-dose CT.
* A P value of <.0083 was considered significant in statistical analysis.

Table 3

Summary of CT quantitative measurements and Bland-Altman analysis for 32 cases of idiopathic interstitial pneumonia.

	Mean ± SD	Bias	P	Limits of agreement
sFBP				
TLV (L)	3.68 ± 1.17	—	—	—
%ILDV (%)	11.84 ± 5.00	—	—	—
uMBIR-Lung				
TLV (L)	3.71 ± 1.17	−0.03	0.31	(−0.34, 0.28)
%ILDV (%)	11.91 ± 5.15	−0.07	0.80	(−3.09, 2.95)
uMBIR-Stnd				
TLV (L)	3.70 ± 1.18	−0.02	0.59	(0.34, 0.30)
%ILDV (%)	12.69 ± 5.57	−0.84	0.013*	(−4.39, 2.71)

%ILDV = percentage of interstitial lung disease volume, FBP = filtered back projection, MBIR = model-based iterative reconstruction, SD = standard deviation, sFBP = FBP on standard-dose CT, TLV = total lung volume, uMBIR-Lung = MBIR with lung setting on ultra-low-dose CT, uMBIR-Stnd = MBIR with conventional setting on ultra-low-dose CT.
Bias was calculated as the difference between sFBP and MBIRs and assessed with t-test. The limit of agreement was calculated by multiplying the SD of the difference between sFBP and MBIRs by 1.96.
* A P value of <.05 was considered significant.
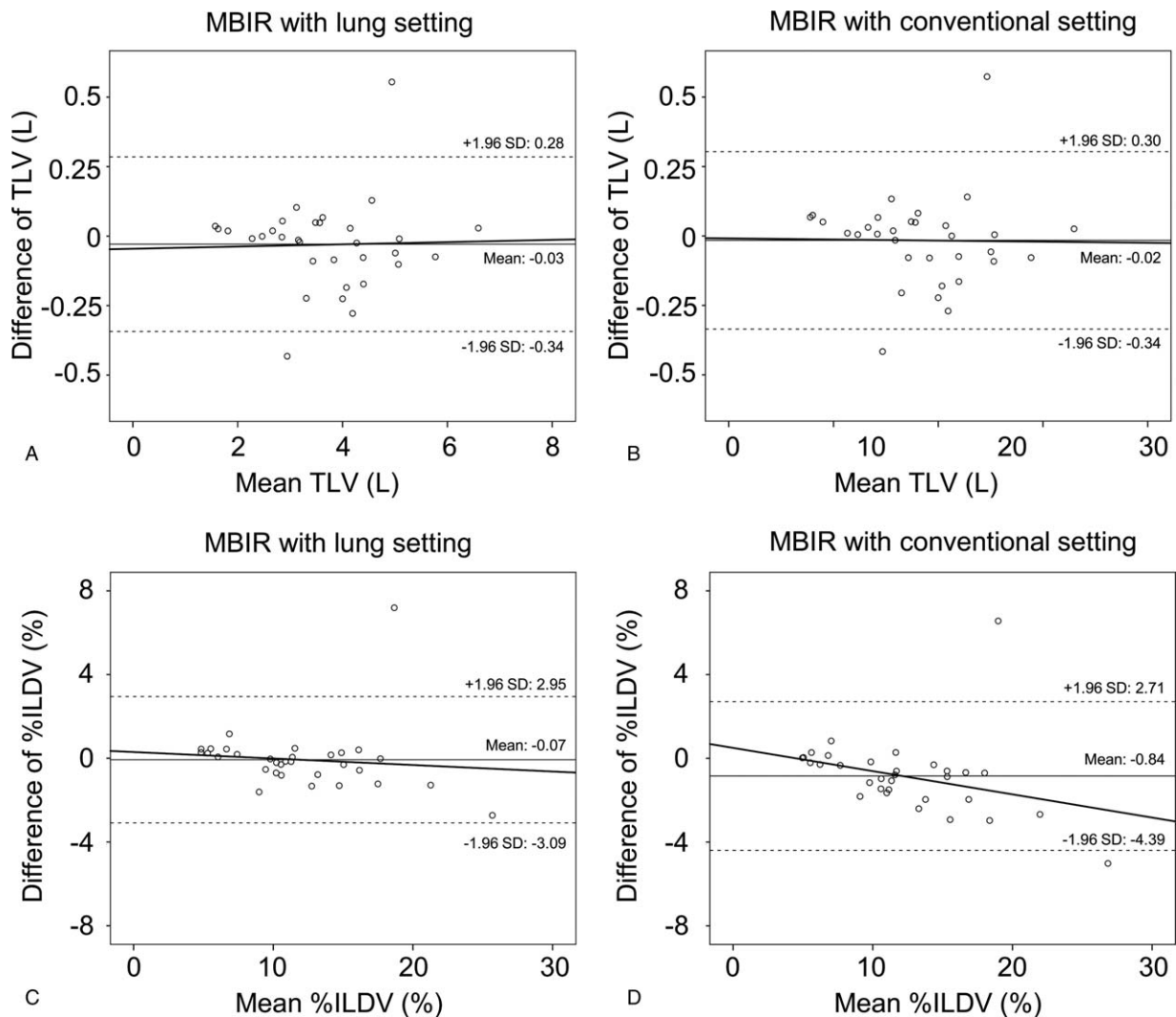
Figure 5. Bland-Altman plots of TLV (A and B) and %ILDV (C and D) comparing MBIRs on ultra-low-dose CT with FBP on standard-dose CT. MBIR with lung setting (a and c) and MBIR with conventional setting (b and d). Solid thin line indicates mean difference (bias). Top and bottom dashed lines correspond to upper and lower margins of limits of agreement. Linear regression lines are indicated as solid bold lines; $y = 0.004 x - 0.046$, $R^2 = 0.001$, and $P = .86$ for (A); $y = -0.002 x - 0.009$, $R^2 < 0.001$, and $P = 0.94$ for (B); $y = -0.031 x + 0.3$, $R^2 = 0.01$, and $P = .58$ for (C); $y = -0.1.11 x + 0.5$, $R^2 = 0.10$, and $P = 0.08$ for (D). CT = computed tomography, FBP = filtered back projection, ILDV = the percentage of interstitial lung disease volume, MBIR = model-based iterative reconstruction, TLV = total lung volume%.

CT. These improvements may solve the previously described disadvantage of MBIR.

For the CT quantitative analysis, FBP on ultra-low-dose CT was inappropriate because of segmentation failure. Excessive image noise on the FBP image on ultra-low-dose CT may prevent successful segmentation. However, the segmentation was successful using MBIR on ultra-low-dose CT and MBIR with the lung setting showed equivalent %ILDV to standard-dose CT. %ILDV has been reported to correlate with the visual extent of ILD or the results of pulmonary function testing.[20] Our result suggests that ultra-low-dose CT using MBIR with the lung setting may be useful for evaluation of extent or progression of ILD. In one case, the bias of %ILDV was >6% in both uMBIR-Lung and uMBIR-Stnd. In this case, TLV was reduced by 14% in both uMBIR-Lung and uMBIR-Stnd compared with sFBP. The separate breath-hold for the ultra-low-dose and standard-dose scan might affect the CT

quantitative measurements. It is necessary to validate our results using spirometry-gated CT.

The image quality of ultra-low-dose CT with MBIR performed worse than that of standard-dose CT, except for noise and streak artifact. In some cases, it was difficult to identify honeycombing on ultra-low-dose CT. Honeycombing is necessary for the diagnosis of the UIP pattern, and the presence of the UIP pattern on CT is sufficient for the diagnosis of idiopathic pulmonary fibrosis according to the international consensus.[29] If the honeycombing is overlooked on CT with poor image quality, an unnecessary surgical lung biopsy may be performed. Thus, ultra-low-dose CT with our protocol may be insufficient for detailed assessment of ILD. However, %ILDV evaluation using MBIR with lung-setting on ultra-low-dose CT showed good agreement with that of standard-dose CT. It is necessary to detect interstitial lesions for screening CT and to evaluate the change of the extent of the lesions at follow-up, but detailed assessment, such as

classification of ILD, is not necessarily needed. For simple assessments such as screening or follow-up of ILD, ultra-low-dose CT with MBIR may be useful clinically.

The present study had several limitations. First, most of the study population had no pathological proof of ILD, and it was not possible to evaluate the diagnostic ability of MBIR on ultra-low-dose CT. Second, although there are some reports of objective analyses for ILD using histogram analysis or texture classification method,[30] those analyses were not performed in this study. We considered that ultra-low-dose CT would be used mainly for screening or follow-up and simple assessments were needed, but our quantitative analysis might be too simple to reflect the accurate extent of the ILD lesion. Third, only a CT scanner and an IR technique developed by a single vendor were used. Differences in CT scanners and IR techniques may show different results, even at the same radiation dose level. Fourth, although analyses were conducted in a blinded manner for reconstruction and radiation dose, MBIRs showed some unique appearances, so complete blinding was difficult. Fifth, only 1 obese patient (BMI $>30 \text{kg/m}^2$) was included in the study, and the protocol was not changed depending on the BMI. Generally, patients with a high BMI need a higher radiation dose to achieve appropriate image quality. The present results cannot be applied to high-BMI patients. Lastly, fixed tube current was used for ultra-low-dose CT, whereas automatic tube current modulation was used for standard-dose CT. Automatic modulation for ultra-low-dose CT was not available at the time of the study. Further investigations are needed to develop the optimal protocol for ultra-low-dose CT.

In conclusion, the lung setting provided more appropriate image quality than the conventional setting for ILD using MBIR on ultra-low-dose CT. Although inferior to standard-dose CT for image quality, MBIR with the lung setting on ultra-low-dose CT showed equivalent CT quantitative measurements to standard dose CT.

Author contributions

Conceptualization: Akinori Hata, Masahiro Yanagawa, Osamu Honda, Noriyuki Tomiyama.
Data curation: Akinori Hata, Masahiro Yanagawa.
Formal analysis: Akinori Hata.
Funding acquisition: Noriyuki Tomiyama.
Investigation: Akinori Hata, Masahiro Yanagawa, Osamu Honda, Tomo Miyata, Noriyuki Tomiyama.
Methodology: Akinori Hata, Masahiro Yanagawa, Osamu Honda, Tomo Miyata, Noriyuki Tomiyama.
Project administration: Akinori Hata.
Resources: Akinori Hata.
Software: Akinori Hata.
Supervision: Masahiro Yanagawa, Osamu Honda, Noriyuki Tomiyama.
Validation: Masahiro Yanagawa, Osamu Honda, Noriyuki Tomiyama.
Visualization: Akinori Hata.
Writing – original draft: Akinori Hata.
Writing – review & editing: Masahiro Yanagawa, Osamu Honda, Tomo Miyata, Noriyuki Tomiyama.

References

[1] Katsura M, Matsuda I, Akahane M, et al. Model-based iterative reconstruction technique for radiation dose reduction in chest CT: comparison with the adaptive statistical iterative reconstruction technique. Eur Radiol 2012;22:1613–23.

[2] Yamada Y, Jinzaki M, Tanami Y, et al. Model-based iterative reconstruction technique for ultralow-dose computed tomography of the lung: a pilot study. Invest Radiol 2012;47:482–9.

[3] Yanagawa M, Gyobu T, Leung AN, et al. Ultra-low-dose CT of the lung. Acad Radiol 2014;21:695–703.

[4] Haggerty JE, Smith Ea, Kunisaki SM, et al. CT imaging of congenital lung lesions: effect of iterative reconstruction on diagnostic performance and radiation dose. Pediatr Radiol 2015;989–97.

[5] Koc G, Courtier JL, Phelps A, et al. Computed tomography depiction of small pediatric vessels with model-based iterative reconstruction. Pediatr Radiol 2014;44:787–94.

[6] Annoni AD, Andreini D, Pontone G, et al. Ultra-low-dose CT for left atrium and pulmonary veins imaging using new model-based iterative reconstruction algorithm. Eur Heart J Cardiovasc Imaging 2015;16:1366–73.

[7] Pickhardt PJ, Lubner MG, Kim DH, et al. Abdominal CT with model-based iterative reconstruction (MBIR): initial results of a prospective trial comparing ultralow-dose with standard-dose imaging. Am J Roentgenol 2012;199:1266–74.

[8] Lubner MG, Pooler BD, Kitchin DR, et al. Sub-milliSievert (sub-mSv) CT colonography: a prospective comparison of image quality and polyp conspicuity at reduced-dose versus standard-dose imaging. Eur Radiol 2015;25:2089–102.

[9] Notohamiprodjo S, Deak Z, Meurer F, et al. Image quality of iterative reconstruction in cranial CT imaging: comparison of model-based iterative reconstruction (MBIR) and adaptive statistical iterative reconstruction (ASiR). Eur Radiol 2014;140–6.

[10] Hérin E, Gardavaud F, Chiaradia M, et al. Use of Model-Based Iterative Reconstruction (MBIR) in reduced-dose CT for routine follow-up of patients with malignant lymphoma: dose savings, image quality and phantom study. Eur Radiol 2015;2362–70.

[11] Boudabbous S, Arditi D, Paulin E, et al. Model-Based Iterative Reconstruction (MBIR) for the Reduction of Metal Artifacts on CT. AJR Am J Roentgenol 2015;205:380–5.

[12] Thibault J-B, Sauer KD, Bouman CA, et al. A three-dimensional statistical approach to improved image quality for multislice helical CT. Med Phys 2007;34:4526–44.

[13] Yasaka K, Katsura M, Hanaoka S, et al. High-resolution CT with new model-based iterative reconstruction with resolution preference algorithm in evaluations of lung nodules: comparison with conventional model-based iterative reconstruction and adaptive statistical iterative reconstruction. Eur J Radiol 2016;85:599–606.

[14] Hata A, Yanagawa M, Honda O, et al. Submillisievert CT using model-based iterative reconstruction with lung-specific setting: an initial phantom study. Eur Radiol 2016;26:4457–64.

[15] Wang R, Sui X, Schoepf UJ, et al. Ultralow-radiation-dose chest CT: accuracy for lung densitometry and emphysema detection. Am J Roentgenol 2015;204:743–9.

[16] Messerli M, Kluckert T, Knitel M, et al. Ultralow dose CT for pulmonary nodule detection with chest x-ray equivalent dose—a prospective intra-individual comparative study. Eur Radiol 2017;27:3290–9.

[17] Huber A, Landau J, Ebner L, et al. Performance of ultralow-dose CT with iterative reconstruction in lung cancer screening: limiting radiation exposure to the equivalent of conventional chest X-ray imaging. Eur Radiol Springer Berlin Heidelberg; 2016;26:3643–52.

[18] Ebner L, Bütikofer Y, Ott D, et al. Lung nodule detection by microdose CT versus chest radiography (standard and dual-energy subtracted). Am J Roentgenol 2015;204:727–35.

[19] Best AC, Meng J, Lynch AM, et al. Idiopathic pulmonary fibrosis: physiologic tests, quantitative CT indexes, and CT visual scores as predictors of mortality. Radiology 2008;246:935–40.

[20] Shin KE, Chung MJ, Jung MP, et al. Quantitative computed tomographic indexes in diffuse interstitial lung disease. J Comput Assist Tomogr 2011;35:266–71.

[21] Camiciottoli G, Orlandi I, Bartolucci M, et al. Lung CT densitometry in systemic sclerosis: correlation with lung function, exercise testing, and quality of life Chest. Am Coll Chest Phys 2007;131:672–81.

[22] Matsuoka S. Objective quantitative CT evaluation using different attenuation ranges in patients with pulmonary fibrosis: correlations with visual scores. Int J Respir Pulm Med 2016;3:

[23] Sverzellati N, Calabrò E, Chetta A, et al. Visual score and quantitative CT indices in pulmonary fibrosis: relationship with physiologic impairment. Radiol Med 2007;112:1160–72.

[24] Medicine AA of P in. AAPM Report No. 96 - The Measurement, Reporting, and Management of Radiation Dose in CT. Am Assoc Phys Med. 2008; 1-34. https://www.aapm.org/pubs/reports/detail.asp?docid=97

[25] Boehm T, Willmann JK, Hilfiker PR, et al. Thin-section CT of the lung: does electrocardiographic triggering influence diagnosis? Radiology 2003;229:483–91.

[26] Mayo JR, Webb WR, Gould R, et al. High-resolution CT of the lungs: an optimal approach. Radiology 1987;163:507–10.

[27] Murata K, Khan A, Rojas KA, et al. Optimization of computed tomography technique to demonstrate the fine structure of the lung. Invest Radiol 1988;23:170–5.

[28] Padole A, Singh S, Ackman JB, et al. Submillisievert Chest CT With Filtered Back Projection and Iterative Reconstruction Techniques. AJR Am J Roentgenol 2014;203:772–81.

[29] Raghu G, Collard HR, Egan JJ, et al. An official ATS/ERS/JRS/ALAT statement: idiopathic pulmonary fibrosis: evidence-based guidelines for diagnosis and management. Am J Respir Crit Care Med 2011;183:788–824.

[30] Jacob J, Bartholmai BJ, Rajagopalan S, et al. Mortality prediction in idiopathic pulmonary fibrosis: evaluation of computer-based CT analysis with conventional severity measures. Eur Respir J 2017;49:1601011.